Computer Simulation of Cosolvent Effects on Hydrophobic Hydration

Paul E. Smith*

Department of Biochemistry, Kansas State University, Manhattan, Kansas 66506-3702

Received: August 6, 1998

The effects of cosolvents on the solubility and hydration of small nonpolar solutes in solution has been investigated using a combination of molecular dynamics simulation and Widom particle insertion calculations. Results were obtained for helium, neon, argon, and methane solutes in solutions of sodium chloride, ammonium sulfate, calcium chloride, ammonium acetate, tetramethylammonium chloride, guanidinium chloride, urea, and TFE. The effects of varying the cosolvent concentration was also investigated for guanidinium chloride, urea, and TFE. The calculated salting out constants were in excellent agreement with experimental data even though the solvation free energy differences were small in magnitude. Analysis of the solvation properties of the solutes in different cosolvents using a preferential binding model indicated that, for low cosolvent concentrations, the degree of preferential cosolvent binding to the solute was the dominant factor in determining the change in free energy of solvation and hence the salting out properties of the cosolvent.

Introduction

Protein folding and protein solubility are two areas of research where hydrophobic hydration and the hydrophobic effect are thought to play a central role.[1−3] Improving our understanding of hydrophobic hydration effects in biological systems will provide the knowledge required to help manipulate many of the physical properties of peptides and proteins. Unfortunately, the properties of peptides and proteins are not only affected by the presence of water but also by other species, commonly referred to as cosolvents, present in solution. Some of these effects arise as a direct consequence of relatively simple modifications of the properties of water, while others appear to be more complicated and specific to particular cosolvents. Even though these effects have been studied in great detail,[4−13] at present no general atomic level picture exists of the effects of different cosolvents on the structure and properties of peptides and proteins.[12]

Commensurate with a realization of the growing importance of cosolvent effects in chemical and biological systems there have been many models and theories developed in an attempt to rationalize cosolvent behavior. A relatively simple model to predict gas solubility in salt solutions has been developed by Schumpe and coworkers.[14−16] Here, solubility constants are decomposed into cation, anion, and gas contributions which are then parameterized using a large dataset. Predictions are good but provide no information as to why certain anions or cations behave in a particular manner. Other parameterized models also exist but suffer from the same drawback.[17,18]

Early theories of salt effects on protein solubility treated the solvent as a continuum and considered the effect of salts on the dielectric permittivity of the solution.[19] Other electrostatic and thermodynamic theories have also been developed.[20−22] However, all these theories treat the ions in a mean field or Debye−Hückel manner. Hence, the theories are limited to low ionic strengths, and specific ion interactions with the solute are not accounted for.[23] The most common and successful model for predicting salt effects on solute solubility is that of scaled particle theory,[24,25] as extended to include salt effects.[26−29] Although scaled particle theory is a thermodynamic technique applied to microscopic cavities, it has provided quantitative agreement with experiment for a wide range of salts. It cannot, however, provide the microscopic picture of salt effects desired in this work. More importantly, it is essentially limited to the study of spherical cavities.

In our initial efforts to rationalize the effects of different cosolvents on peptide and protein structure and dynamics we have chosen to focus on the effects of cosolvents on the properties of small nonpolar solutes. These systems serve as a model for understanding the role of cosolvents in the hydrophobic effect and have been chosen for several reasons. First, even small peptides are complex mixtures of many different functional groups, some or all of which may interact with solvent and cosolvents in a variety of ways. Deconvolution of these many effects is impossible at this time, and smaller model systems are therefore necessary. Second, quantitative experimental data is available characterizing the effects of cosolvents on the solubility of nonpolar molecules in solution. Our results can be compared directly with experiment to determine if currently available cosolvent force fields are accurate enough to be used in more elaborate studies. Third, high precision results can be obtained for the free energy of solvation of small solutes in solution using standard computer simulation techniques, which also provide an atomic level picture of changes in hydrophobic hydration in the presence of different cosolvents. Finally, it is well-known that the temperature dependent solubilities of small nonpolar molecules mimic the major features of protein unfolding.[30−32] In addition, denaturing agents, such as urea and guanidinium chloride, are known to interact as strongly with nonpolar groups as they do with peptide groups,[33] although their exact mechanism of action still remains unclear.[34,35] These observations suggest that a study of the hydration properties of small nonpolar molecules may offer valuable insights into the protein folding/unfolding mechanism.

While many simulations have been performed to determine the underlying details of the hydrophobic effect (see ref 1 and

* To whom correspondence should be addressed. Fax: 785-532-7278. E-mail: pesmith@ksu.edu.

10.1021/jp983303c CCC: $18.00
Published on Web 12/30/1998

references therein), most investigations have focused on the hydration properties of nonpolar molecules,[36−39] calculating potentials of mean force between hydrophobic molecules,[40−45] or calculating potentials of mean force between nonpolar molecules and cosolvents.[46,47] Some recent studies have begun to probe the effects of salts and cosolvents on the properties of nonpolar molecules at infinite dilution.[45,48,49] Kinoshita and Hirata performed an integral equation study of salt effects on the solubility of noble gases.[48] They observed that strongly hydrated ions (F^-, Li^+, and Na^+) are excluded from the vicinity of the noble gas while other ions (Cl^- and Br^-) are excluded from the bulk solution. They also found that cations affect the solubility of noble gases indirectly, whereas anions have both an indirect and direct effect on the solute. However, experimental salting out constants were significantly overestimated. Recently, the potential of mean force between two methane molecules in pure water and 6 M urea has been investigated by Wallqvist et al.[45] They observed a stabilization of the methane−methane contact pair in the presence of high concentrations of urea.[45] However, to our knowledge, no systematic simulations studies have been performed to investigate the nature of cosolvent modifications of hydrophobic hydration.

The nonpolar solutes chosen for this study were helium, neon, argon, and methane. The cosolvents studied were sodium chloride, ammonium sulfate, calcium chloride, ammonium acetate, tetramethylammonium chloride, guanidinium chloride (GdmCl), urea, and 2,2,2-trifluoroethanol (TFE). The above cosolvents were chosen as they are known to produce a wide range of effects on peptides and proteins including; salting in/out effects, denaturing effects, and secondary structure stabilizing effects. In addition, force field parameters are currently available for all the above cosolvents. In the case of urea, guanidinium chloride and TFE we have also studied the effects of varying the cosolvent concentration. The overall approach was to perform long molecular dynamics simulations of the cosolvent/solvent systems, followed by Widom particle insertion calculations to determine the solvation free energy for each solute into each cosolvent system.

Methods

Classical molecular dynamics simulations in water and in water plus cosolvent were performed. Nonbonded parameters were taken from current literature values (see Table 1). Intramolecular parameters were taken from the same source were possible, or from the CHARMM22 force field[50] for analogous compounds. Initial cosolvent configurations were generated from a cubic box ($L \approx 2.5$ nm) of 512 equilibrated water molecules by randomly replacing waters with cosolvent to attain the required cosolvent concentration, minimizing with 100 steps of steepest descent, followed by extensive equilibration (see Table 2). Initial equilibration of the system was performed for 1 ns. The equilibration was then continued until all interspecies potential energy contributions displayed no drift with time. Simulations were performed in the N, p, T ensemble at 300 K and 1 atm using the weak coupling technique to modulate the temperature and pressure,[51] with relaxation times of 0.1 and 0.5 ps, respectively. SHAKE[52] was used to constrain all bonds with a relative tolerance of 10^{-4}, allowing a 2 fs time step for integration of the equations of motion. Total simulation times were in the 2−5 ns range, the final nanosecond of which was used for calculating ensemble averages. Electrostatic interactions were calculated using the Ewald technique,[53] using a convergence parameter of 2.5 nm^{-1}, a real space cutoff of 1.2 nm, and including all lattice vectors with $n^2 \leq 49$. Configurations were saved every 0.1 ps for the particle insertion calculations. For a system of this size our code requires 10 min/ps on a DEC Personal Workstation (EV5/600 Mhz). Widom particle insertion runs were performed using a total of 10^9 insertions equally divided between 10^4 configurations covering a simulation time of 1ns using the solute parameters given in Table 1. Further details are given in the appendix. Statistical mechanical perturbation theory was used to calculate radial distribution functions in the perturbed ensemble according to[54,55]

$$\langle A \rangle_{N+1,p,T} = \frac{\langle AV e^{-\beta \Delta U} \rangle_{N,p,T}}{\langle V e^{-\beta \Delta U} \rangle_{N,p,T}} \quad (1)$$

where A can be any property of interest, $\beta = (k_B T)^{-1}$, ΔU is

TABLE 1: Nonbonded Force Field Parameters[a]

species	atom	q |e|	ϵ, kJ/mol	σ, nm	ref
water (SPC/E)	O	−0.8476	0.6506	0.3166	79
	H	0.4238	0.0		
helium	He	0.0	0.0850	0.2280	80
neon	Ne	0.0	0.3910	0.2720	80
argon	Ar	0.0	0.9960	0.3410	80
methane	CH_4[b]	0.0	1.2310	0.3730	81
Na^+	Na	1.0000	0.2340	0.2850	82
Ca^{2+}	Ca	2.0000	0.5069	0.2813	82
NH_4^+	N	−0.8960	0.8368	0.3385	83
	H	0.4740	0.0		
$N(CH_3)_4^+$	N	0.0	0.7113	0.3250	66
	CH_3[b]	0.2500	0.6067	0.3960	
Gdm^+	N	−0.8000	0.7113	0.3250	84
	C	0.6400	0.2092	0.2250	
	H	0.4600	0.0		
Cl^-	Cl	−1.0000	0.5380	0.3750	82
SO_4^{2-}	S	2.0000	1.0460	0.3550	67
	O	−1.0000	0.8368	0.3150	
AcO^-	C	0.7000	0.4393	0.3750	66
	O	−0.8000	0.8786	0.2960	
	CH_3[b]	−0.1000	0.6694	0.3910	
urea	C	0.1420	0.4393	0.3750	46
	O	−0.3900	0.8786	0.2960	
	N	−0.5420	0.7113	0.3250	
	H	0.3330	0.0		
TFE	CH_2[b]	0.2600	0.4896	0.3920	85
	CF_3	0.5900	0.4059	0.3361	
	O	−0.5500	0.8496	0.2955	
	F	−0.2000	0.5538	0.3050	
	H	0.3000	0.0		

[a] Symbols are q, atomic charge; ϵ and σ, Lennard-Jones 6−12 well depth and diameter, respectively. The geometric mean was used for both ϵ and σ combining rules. [b] United atom carbons.

TABLE 2: Summary of the Molecular Dynamics Runs[a]

system	cosolvent	N_c	N_w	$\langle V \rangle$, nm^3	C_c, mol/L	A_c	T_{sim}, ns
0	none	0	512	15.419			2.0
1	NaCl	9	494	14.937	1.001	0.01	4.0
2	$(NH_4)_2$ SO_4	9	485	15.460	0.967	0.00	5.0
3	$CaCl_2$	9	485	14.520	1.029	0.03	3.0
4	NH_4OAc	9	494	15.246	0.980	0.00	2.0
5	$N(CH_3)_4Cl$	9	494	16.174	0.924	−0.02	2.0
6	GdmCl	9	494	15.630	0.956	−0.01	3.0
7	urea	9	503	15.795	0.946	−0.01	3.0
8	TFE	9	476	15.352	0.973	−0.02	2.0
9	GdmCl	50	350	15.321	5.418	−0.10	2.0
10	urea	50	400	15.461	5.307	−0.06	2.0
11	TFE[b]	40	360	15.603	4.257	−0.11	2.5
12	urea	75	350	15.567	7.999	−0.08	2.0

[a] N_c, number of cosolvent molecules; N_w, number of water molecules; $\langle V \rangle$, average volume of the solution; C_c, cosolvent concentration; $A_c = \log (\sum_i \rho_i / \sum_i \rho_i^0)$, see eq 3; T_{sim}, total simulation time. [b] Approximately 30% by volume.

TABLE 3: Cavity Insertion Results for Helium[a]

cosolvent	C_c, mol/L	ΔG, kJ/mol	ΔH, kJ/mol	$\Delta G - \Delta G_0$, kJ/mol	k_c, L/mol	k_c^{exp}, L/mol
none		7.06(3)	−1(1)			
NaCl	1.001	7.58(4)	0.1(1)	0.52(5)	0.10(1)	0.09
$(NH_4)_2SO_4$	0.967	7.68(3)	0.7(3)	0.62(4)	0.11(1)	
$CaCl_2$	1.029	7.97(1)	0.7(5)	0.91(3)	0.18(1)	
NH_4OAc	0.980	7.38(3)	0.4(3)	0.32(4)	0.06(1)	
$N(CH_3)_4Cl$	0.924	7.14(1)	0.4(5)	0.08(3)	−0.01(1)	
GdmCl	0.956	7.38(3)	0.2(4)	0.32(4)	0.05(1)	
urea	0.946	7.17(2)	0.1(9)	0.11(4)	0.01(1)	
TFE	0.973	7.11(0)	0.6(4)	0.05(3)	−0.02(1)	
GdmCl	5.418	8.37(6)	2.0(4)	1.31(7)	0.02(0)	
urea	5.307	7.71(2)	0.8(9)	0.65(4)	0.01(0)	
TFE	4.257	6.95(3)	1.7(4)	−0.11(4)	−0.03(0)	
urea	7.999	8.05(5)	1(1)	0.99(6)	0.01(0)	

[a] C_c, cosolvent concentration; ΔG, excess solvation free energy; ΔH, excess enthalpy of solvation; k_c, salting out parameter. Values in parentheses denote the standard deviation in the last digit. Experimental values were taken from ref 86.

TABLE 4: Cavity Insertion Results for Neon[a]

cosolvent	C_c, mol/L	ΔG, kJ/mol	ΔH, kJ/mol	$\Delta G - \Delta G_0$, kJ/mol	k_c, L/mol	k_c^{exp}, L/mol
none		8.29(6)	−4(2)			
NaCl	1.001	9.04(6)	−3(1)	0.75(8)	0.14(1)	0.12
$(NH_4)_2SO_4$	0.967	9.10(5)	−1(1)	0.81(8)	0.15(1)	
$CaCl_2$	1.029	9.56(3)	−1(1)	1.27(7)	0.24(1)	0.22
NH_4OAc	0.980	8.72(6)	−2(1)	0.43(8)	0.08(1)	
$N(CH_3)_4Cl$	0.924	8.37(2)	−2(1)	0.08(6)	−0.01(1)	
GdmCl	0.956	8.69(8)	−3(1)	0.40(9)	0.06(2)	
urea	0.946	8.39(4)	−2(2)	0.10(7)	0.01(1)	0.02
TFE	0.973	8.28(2)	−1(1)	−0.01(6)	−0.02(1)	
GdmCl	5.418	9.9(2)	1(1)	1.6(2)	0.03(1)	
urea	5.307	8.95(3)	−2(2)	0.66(7)	0.01(0)	0.02
TFE	4.257	7.67(6)	0(1)	−0.62(8)	−0.05(0)	
urea	7.999	9.30(8)	−2(3)	1.0(1)	0.01(0)	0.02

[a] See Table 3 for footnotes. Experimental values were taken from ref 87.

the change in configurational energy on insertion of the cavity, and the angular brackets denote an ensemble average. Inclusion of the system volume V arises when considering particle insertion in the N, p, T ensemble (see Appendix).[55] For polyatomic solvents and cosolvents, the center of mass was used to determine the position of the species of interest. Standard deviations were estimated by determining properties from four subaverages spanning 250 ps each.

Results

(i) Solvation Free Energies. The free energy of solvation for the four different solutes in each of the different solvent and cosolvent systems are presented in Tables 3−6. The solvation free energies for the solutes helium, neon, argon and methane in pure water at infinite dilution (7.1, 8.3, 9.0, and 9.4 kJ/mol, respectively) do not compare well with the corresponding experimental values of 11.6, 11.2, 8.4, and 8.4 kJ/mol, respectively (from refs 56 and 57 corrected to infinite dilution[38]). In fact, the experimental trend displays a decrease in solvation free energy with solute size, while the calculations predicted an increase. This behavior has been observed in previous simulation studies,[38,48] and the experimental trend seems to be reproduced when polarization effects are included in the calculations.[36] The role of polarization in determining salting out effects is beyond the scope of the current work. Fortunately, as we were mainly interested in differences between free energies of solvation, it is reasonable to assume that polarization

TABLE 5: Cavity Insertion Results for Argon[a]

cosolvent	C_c, mol/L	ΔG, kJ/mol	ΔH, kJ/mol	$\Delta G - \Delta G_0$, kJ/mol	k_c, L/mol	k_c^{exp}, L/mol
none		9.0(2)	−9(5)			
NaCl	1.001	10.2(1)	−7(2)	1.2(2)	0.22(3)	0.15
$(NH_4)_2SO_4$	0.967	10.1(1)	−2(4)	1.1(2)	0.20(4)	
$CaCl_2$	1.029	10.7(2)	11(6)	1.7(3)	0.32(5)	
NH_4OAc	0.980	9.6(1)	−7(3)	0.6(2)	0.11(4)	
$N(CH_3)_4Cl$	0.924	9.2(1)	−6(4)	0.2(2)	0.02(4)	0.02[b]
GdmCl	0.956	9.5(2)	−8(1)	0.5(3)	0.08(5)	
urea	0.946	9.1(2)	−6(7)	0.1(3)	0.01(6)	
TFE	0.973	8.9(7)	−3(2)	−0.1(7)	−0.04(9)	
GdmCl	5.418	10.7(5)	2(8)	1.7(5)	0.04(2)	
urea	5.307	9.5(1)	−8(4)	0.5(2)	0.01(1)	
TFE	4.257	7.0(1)	−3(4)	−2.0(2)	−0.11(1)	
urea	7.999	9.9(2)	−8(8)	0.9(3)	0.01(1)	

[a] See Table 3 for footnotes. Experimental values were taken from ref 87. [b] From ref 28.

TABLE 6: Cavity Insertion Results for Methane[a]

cosolvent	C_c, mol/L	ΔG, kJ/mol	ΔH, kJ/mol	$\Delta G - \Delta G_0$, kJ/mol	k_c, L/mol	k_c^{exp}, L/mol
none		9.4(3)	−11(9)			
NaCl	1.001	10.7(2)	−8(3)	1.3(4)	0.24(7)	0.16
$(NH_4)_2SO_4$	0.967	10.6(1)	−13(5)	1.2(3)	0.22(5)	0.24
$CaCl_2$	1.029	11.2(4)	1(11)	1.8(5)	0.33(8)	0.26
NH_4OAc	0.980	10.0(2)	−12(5)	0.6(4)	0.11(7)	
$N(CH_3)_4Cl$	0.924	9.7(2)	−8(7)	0.3(4)	0.03(8)	
GdmCl	0.956	9.8(3)	−11(1)	0.4(4)	0.06(7)	0.03
urea	0.946	9.4(4)	−8(11)	0.0(5)	−0.01(9)	0.01
TFE	0.973	9.2(1)	−3(5)	−0.2(3)	−0.06(6)	
GdmCl	5.418	11.0(7)	5(17)	1.6(8)	0.03(3)	0.03
urea	5.307	9.8(1)	−13(5)	0.4(3)	0.00(1)	0.01
TFE	4.257	6.6(2)	−5(7)	−2.8(4)	−0.14(0)	
urea	7.999	10.4(2)	−10(9)	1.0(3)	0.01(1)	0.01

[a] See Table 3 for footnotes. Experimental values were taken from ref 88.

effects will be similar for all cosolvents and will therefore cancel.[48] However, we note that this might not be a good approximation for cosolvents which interact directly with specific solutes. Additionally, it has been assumed that any quantum effects associated with the helium atom will also cancel. Despite the relatively poor agreement with experiment, our solvation free energies are in good agreement with other nonpolarizable studies.[37,38,48,49,58−60]

From Tables 3−6 one finds that the differences between the free energy for insertion into pure water and into water plus cosolvent were very small, often less than 1 kJ/mol. Fortunately, the precision of the free energy calculations was extremely high. Enthalphy and entropy estimates were not so reliable. This may have been a consequence of performing the calculations in the N, p, T ensemble where slow volume fluctuations might delay the convergence of these properties. Particle insertion results for the N, V, E ensemble appear less problematic.[36] As expected, the errors associated with the particle insertion calculation increased with cavity size. To a certain extent one can reduce the errors by simply performing more trial insertions (see Appendix), although eventually it becomes more practical to use thermodynamic integration techniques. All the cosolvents examined here, with the exception of TFE, produced an increase in the excess free energy of solvation associated with cavity formation.

(ii) Salting Out Constants. Salting out constants (k_c) are defined by the Setschenow equation[27]

$$k_c C_c = \log\left(\frac{X_0}{X}\right) \qquad (2)$$

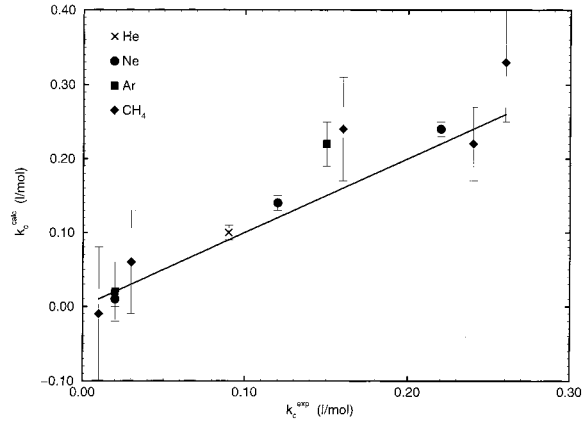

Figure 1. Calculated *versus* experimental salting out coefficients of helium, neon, argon, and methane from different cosolvent solutions. Error bars are ±1 standard deviation. Errors in the experimental salting out constants are typically ±0.01 L/mol.

where C_c is the cosolvent concentration and X is the mole fraction solubility of the solute. The subscript 0 denoting the value obtained in pure solvent. Positive values of k_c indicate a decrease of solubility in the presence of cosolvent, i.e., a salting out effect. Experimental salting out constants are observed to be independent of C_c for most salts up to 1−2 M,[5] but not necessarily for denaturing concentrations of urea or guanidinium chloride. Assuming that k_c is independent of C_c and that the solute solubility is low,[25] one can express the above equation in terms of solvation free energies,[26,27]

$$k_c C_c = \frac{(\Delta G - \Delta G_0)}{2.303RT} + \log\left(\frac{\sum_i \rho_i}{\sum_i \rho_i^0}\right) \qquad (3)$$

where ΔG is the excess solvation free energy ($\mu-\mu^{id}$, see Appendix), R is the gas constant, T the absolute temperature, and ρ_i is the number density of species i, with the subscript or superscript 0 again denoting values obtained in pure solvent. The first term on the right-hand side of eq 3 represents the actual work required to create the cavity, while the second term accounts for changes in system density between the two processes.

From Tables 3−6 one finds that the salting in/out effect increased with increasing cavity size as observed experimentally. The largest salting out effects were observed for sodium chloride, ammonium sulfate and calcium chloride, while TFE produced the only significant salting in effect. A comparison of experimental and calculated salting out constants is presented in Figure 1. The agreement with experiment was excellent considering the small magnitude of many of the corresponding free energy differences. In this respect, agreement with experiment was probably aided by the fact that one is observing differences in free energy differences where errors in single free energies of solvation become less important. These results suggest that (i) a combination of molecular dynamics simulations and particle insertion techniques can provide quantitative information concerning the effects of cosolvents on the solubility of small nonpolar molecules in solution and (ii) that the cosolvent parameters used in the above calculations are capable of reproducing the available experimental data. The predicted salting out constants represent an improvement on previous integral equation predictions.[48]

(iii) Radial Distribution Functions. In an attempt to elucidate which factors were responsible for particular salting in/out effects, we have determined the radial distribution functions (rdfs) between the inserted solutes and different cosolvent species. Figures 2−4 show the rdfs between helium or methane and the cations, anions and neutral cosolvents, respectively. The results for neon and argon (not shown) were consistently observed to lie between that of helium and methane and we have therefore limited the following discussion to the two extreme cases. The distribution of sodium and calcium cations around the solutes appeared to be essentially random

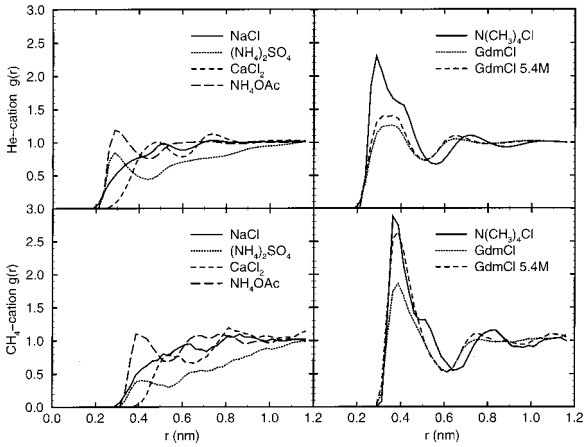

Figure 2. Radial distribution functions between the inserted helium and methane solutes and different cations. Concentrations are 1 M unless otherwise stated.

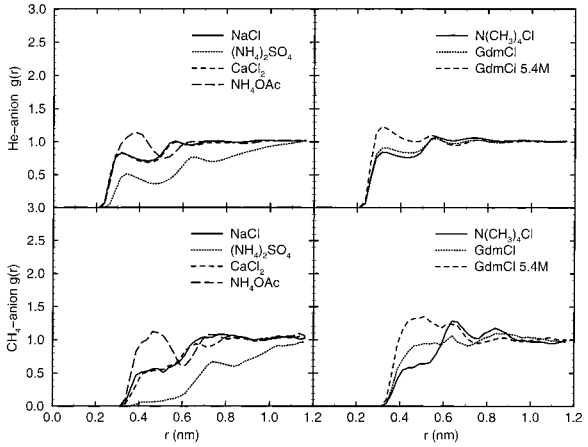

Figure 3. Radial distribution functions between the inserted helium and methane solutes and different anions. Concentrations are 1 M unless otherwise stated.

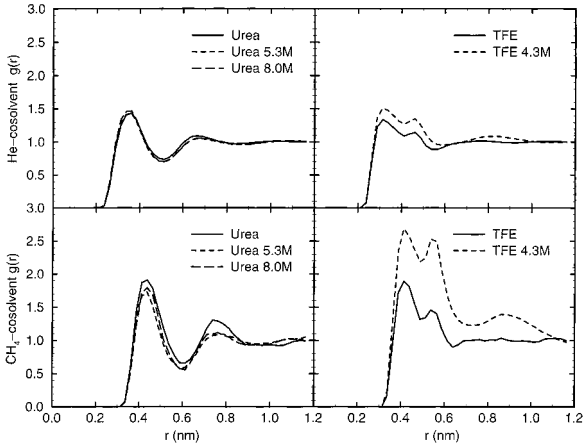

Figure 4. Radial distribution functions between the inserted helium and methane solutes and neutral cosolvents. Concentrations are 1 M unless otherwise stated.

(see Figure 2). For sodium cations, the probability of direct cavity−cation interactions was low, but not zero. Calcium cations, which have similar σ parameters to sodium cations, displayed no direct cavity−cation interactions. This difference probably reflects the much stronger binding of the first solvation shell waters to the calcium cation. The distribution of ammonium cations around the inserted cavities displayed some dependence on the associated anion. Cations of ammonium sulfate were less likely to be found close to the cavity than cations of ammonium acetate. In the case of ammonium sulfate, there was also some dependence on cavity size with the larger cavity displaying an increased degree of cation exclusion.

The distribution of tetramethylammonium and guanidinium cations around the inserted cavities was very different to the other cations. Both cations displayed a strong direct interaction with the larger methane cavity and a somewhat diminished, but still significant, interaction with the helium cavity. The effect of guanidinium cations was concentration dependent, displaying an increased cavity−cation interaction as the cation concentration was increased. Interestingly, the tetramethylammonium and the 5.4 M guanidinium cations displayed almost exactly the same cavity−cation distribution.

The corresponding cavity−anion distributions are displayed in Figure 3. The chloride anions were almost exclusively excluded from the vicinity of a cavity, although this effect appeared to be only minor. The acetate anion distribution was essentially random while the sulfate anion displayed the expected high degree of exclusion.[9] The exclusion of sulfate anions was more pronounced for the larger methane cavity. The chloride anion distribution displayed some dependence on the cation. In particular, the chloride ion distribution in 5.4 M guanidinium chloride increased to where there was a slight excess of chlorides close to the inserted cavities.

The distribution of neutral cosolvents around the inserted cavities is presented in Figure 4. The urea distribution was independent of concentration for the helium cavity. However, the probability of finding a urea molecule close to the larger methane cavity decreased with increasing urea concentration. The distribution of TFE molecules around the helium cavity increased slightly on increasing the cosolvent concentration. This increase was substantially larger in the case of the methane cavity resulting in a large excess of TFE molecules in the vicinity of the cavity. Further decomposition of the TFE distribution indicated that the fluoro groups were providing the major stabilizing interactions with the inserted cavity (data not shown). This agrees well with the proposed mode of action of TFE in stabilizing peptide conformations in solution—the so-called "teflon coat" model.[61]

(iv) Kirkwood−Buff Integrals. In order to quantify some of the data presented in Figures 2−4 we have used the rdfs obtained from the simulations to calculate Kirkwood−Buff (KB) integrals defined as[62]

$$G_{ij} = 4\pi\int_0^{\infty}[g_{ij}(r) - 1]r^2\,\mathrm{d}r \qquad (4)$$

Here, G_{ij} is the Kirkwood−Buff (KB) integral between species i and j, $g_{ij}(r)$ is the corresponding radial distribution function, and the upper integration limit has been truncated at half the box length. A KB integral greater than zero indicates an excess of species j in the vicinity of species i (over a random distribution), while a negative value depicts a depletion of species j surrounding i. We note that KB integrals tend to be slightly negative due to the excluded volume effect of the cavities.

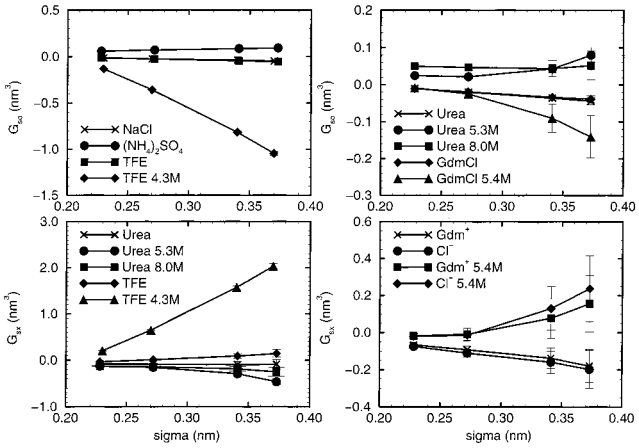

Figure 5. Kirkwood−Buff integrals between (i) the different solutes and water oxygen (top) and (ii) the different solutes and species X (bottom) plotted as a function of solute size, σ. Error bars are ± 1 standard deviation. Concentrations are 1 M unless otherwise stated.

From Figure 5 it is clear that all effects increased in magnitude with increasing cavity size. Ammonium sulfate significantly increased the degree of hydration of all the cavities in solution. This is consistent with the large preferential exclusion of the sulfate anion and an increased surface tension effect.[12] Sodium chloride would also be expected to act in a similar fashion. In fact, the calculated salting out parameters for the two salts were identical within the precision of the current data. However, in Figure 5 we find that sodium chloride did not produce an excess hydration of the cavity in either an absolute sense or with respect to the degree of hydration in pure water (data not shown). It appears that either the two salts display similar salting out effects but by different mechanisms or that the degree of hydration is not a good measure of salting out ability.

To test the first hypothesis, we calculated the rdfs between the different species in 1 M sodium chloride and 1 M ammonium sulfate solutions. The ammonium sulfate solution displayed an unusual liquid state structure. The rdfs for this solution are displayed in Figure 6. There was an extremely high percentage of cation−anion ion pairs observed. In fact, nearly all (90%) of the ammonium and sulfate ions formed contact ion pairs with an oppositely charged ion leading to the formation of a large aggregate of ions which appeared to exclude water from its center. Solvation of the ions by water was correspondingly reduced (see Figure 6) with integration past the first peak giving 2.5 and 7.5 hydration waters for the ammonium and sulfate ions, respectively. However, there was still a substantial first solvation peak in both cases. The aggregation observed here occurred even though the initial configuration was a set of random ion coordinates. Due to formation of this aggregate, equilibration of the system was slow and required over 4 ns of simulation time. The simulation conditions were well below the 5.3 M experimental solubility limit of ammonium sulfate,[63] and the aggregate did not appear to resemble the crystal structure of ammonium sulfate;[64,65] although a direct comparison was difficult due to the relatively low number of ions used in the simulation. Of course, the structure could be an artifact of the potentials chosen. However, the ammonium ion nonbonded parameters are very similar to other models,[47,66] and the sulfate parameters have been developed using usually reliable free energy simulations.[67] Unfortunately, comparison with experimental data concerning the structure of ammonium sulfate solutions is problematic due to the difficulty modeling ammonium ion density.[68] Hence, diffraction studies of sulfate hydration produce sulfate hydration numbers varying between

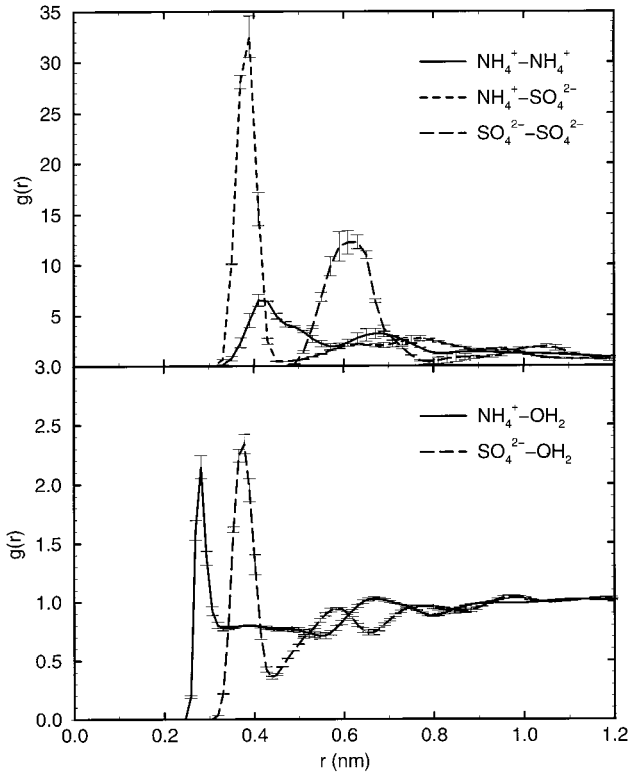

Figure 6. Radial distribution functions obtained for a solution of 1 M ammonium sulfate. Error bars are ±1 standard deviation.

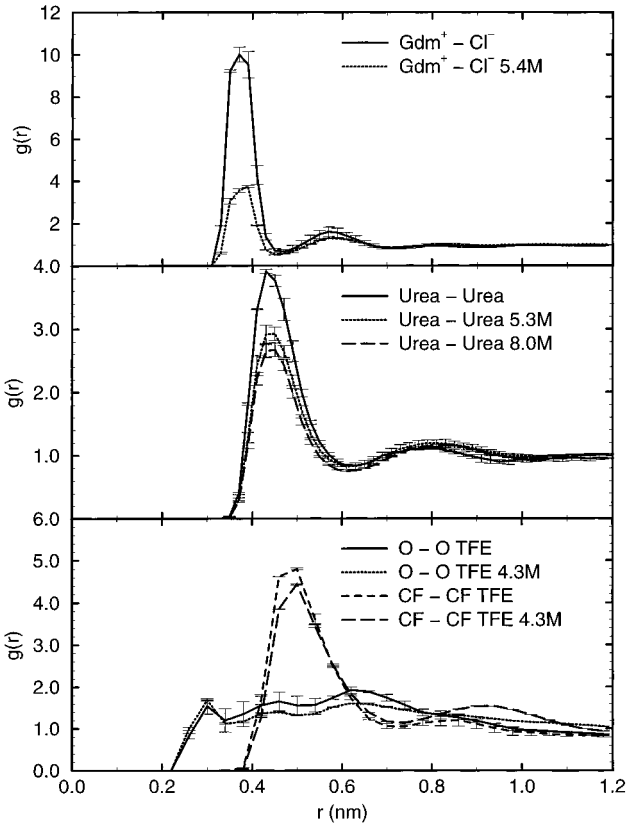

Figure 7. Radial distribution functions obtained for solutions of GdmCl (top), urea (middle), and TFE (bottom) as a function of cosolvent concentration. Error bars are ±1 standard deviation. Concentrations are 1 M unless otherwise stated.

6 and 14.[69] The value obtained for the aggregate observed here (7.5) is within those bounds. The sulfate diffusion constant was reduced to 1.0×10^{-9} m^2 s^{-1} from the value of 1.5×10^{-9} m^2 s^{-1} determined during the original parametrization. We could not find a value for the experimental diffusion constant for comparison. Considering that the ammonium sulfate results do not conflict with any of the available experimental data, and that the salting out constant for methane is very well reproduced, it appears there is no obvious reason to doubt that these aggregates may indeed exist in aqueous ammonium sulfate solutions. Clearly, further study is warranted to clarify this picture.

Figure 5 also compares and contrasts the properties of urea and guanidinium chloride cosolvents. Both cosolvents displayed the same characteristics at low concentrations, i.e., slight exclusion of cosolvent from the vicinity of a cavity, with the hydration of the cavities being essentially the same as that in pure water. However, their effects differed on increasing the cosolvent concentration. While concentrated urea solutions increased the degree of cavity hydration, concentrated guanidinium chloride solutions produced a decrease in cavity hydration. The distribution of cosolvent around the cavities changed correspondingly exhibiting an increased exclusion of urea from the cavity and an increase in the presence of both guanidinium cations and chloride anions close to all the cavities studied here. Changes in the structure of pure urea and guanidinium chloride solutions with concentration are displayed in Figure 7. The urea−urea distribution became less ordered on increasing the urea concentration. The same effect was observed for the cation−anion distributions in guanidinium chloride solutions with the probability of forming a guanidinium−chloride ion pair being higher in the 1 M solution than in the 5.4 M solution (the other ion−ion distributions remained unchanged). This suggests that a sufficient number of waters molecules (per anion or cation) must be present in order to form a significant number of contact ion pairs. The decrease in the number of ion pairs with an increase in cosolvent concentration may help to explain why hydrocarbon solubility in guanidinium chloride solution increases dramatically when the concentration exceeds 3−4 M.[33] Only at high concentrations would the guanidinium ions be free to interact directly with solutes in solution.

TFE desolvated and interacted directly with all the cavities studied here (see Figure 5). The effect was increased substantially on increasing the cosolvent concentration, far more than that observed for high concentrations of urea or guanidinium chloride. The distribution of TFE molecules in solution is shown in Figure 7 as a function of concentration. Here, the TFE molecules interacted more favorably through the trifluoro groups than the hydrogen bonding hydroxyl groups. Unlike urea and guanidinium chloride, the TFE distributions did not change significantly with TFE concentration.

Although no quantitative correlations between salting in/out ability and the degree of hydrophobic hydration are immediately evident from the above results, a general picture does emerge. Strongly excluded cosolvents (sodium chloride, ammonium sulfate and calcium chloride) give rise to large salting out effects. These effects are moderated when the cosolvent interacts favorably with the solute (guanidinium chloride, tetramethylammonium chloride, and urea), and can be reversed if the interaction is strong enough (TFE). For the salts considered here, favorable interactions with a solute exclusively involved the cations.

(v) Preferential Binding Model. The preferential binding model has been used to relate the effects of cosolvents on the unfolding equilibria of proteins to the number of bound cosolvent molecules.[34] The core relationship being

$$\Delta\nu_c^{\text{pref}} = \frac{\partial \ln K}{\partial \ln a_c} \tag{5}$$

where $\Delta\nu_c^{\text{pref}}$ represents the change in the excess number of bound cosolvent molecules (over the number bound considering the cosolvent molecules to be distributed randomly in solution) between the initial and final states of the process, K is the equilibrium constant for the process, and a_c is the activity of the cosolvent. Substituting our solvation process for the above reaction via the simple expression $\Delta G^\circ = -RT \ln K$,[34] then making a finite difference approximation for the above derivative assuming the activity is equal to the concentration, one obtains the following expression

$$\Delta\nu_c^{\Delta G} = -\frac{\Delta G - \Delta G_0}{RT} \tag{6}$$

which relates changes in the preferential binding of cosolvents to differences in the excess free energies of solvation. An expression for $\Delta\nu_c^{\text{pref}}$ can also be obtained directly from the appropriate KB integral

$$\Delta\nu_c^{\text{KB}} = \rho_c G_{sc} \tag{7}$$

where G_{sc} is the KB integral between the solute and the cosolvent and ρ_c is the cosolvent number density. Hence, the above equations represent a direct link between the changes in free energy of solvation and the excess number of cosolvent molecules surrounding the inserted solute.

We have compared the preferential binding numbers obtained directly from the free energy changes (eq 6) with the corresponding values obtained from the radial distribution functions (eq 7). The results are displayed in Figure 8. Values of ρ_c and G_{sc} have been determined assuming that the anions and cations were indistinguishable. From Figure 8 one observes that the agreement between the two expressions was very good for both helium and methane with the exception of ammonium sulfate and cosolvents at high concentrations. The ammonium sulfate data was probably affected by the presence of the ionic aggregate mentioned previously, which could present numerical difficulties when integrating the appropriate rdf. Numerical difficulties might also be a concern for the high concentration cosolvents as the respective rdfs were still oscillating at the upper integration limit of half the box length (see Figures 2−4). The poor agreement for the cosolvents at high concentrations is also to be expected considering some of the approximations made in deriving eq 6. It is interesting to note that the KB integrals appeared to provide a significant increase in precision over the free energy approach. The majority of the cosolvents were preferentially excluded from the solutes. The exceptions were TFE (helium and methane) and guanidinium chloride (methane) at high concentrations. The degree of preferential exclusion was small with a maximum value of 1 cation or anion for the case of calcium chloride around methane. In general, exclusion was 3 times larger for methane than that for helium.

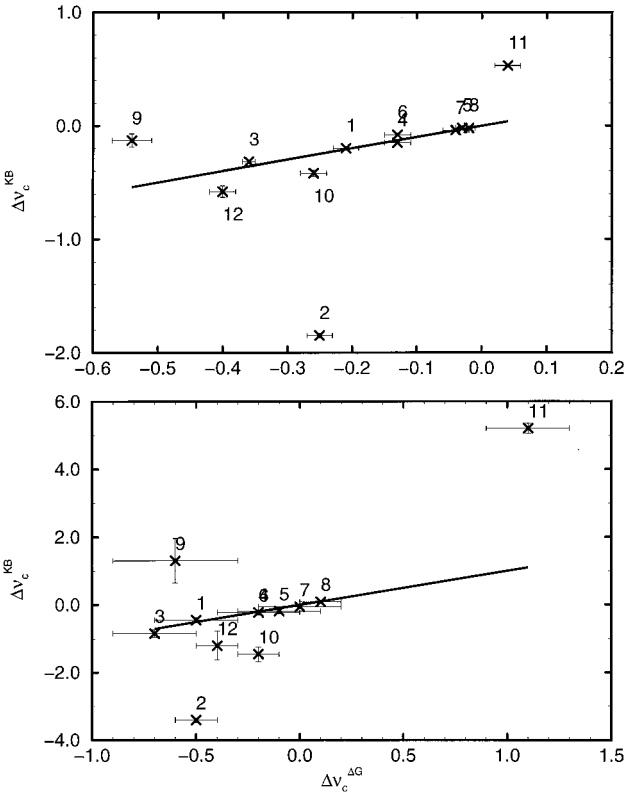

Figure 8. A comparison of the degree of preferential binding of cosolvent obtained for the helium (top) and methane (bottom) solutes using the Kirkwood−Buff approach ($\Delta\nu_c^{\text{KB}}$, eq 7) and the change in solvation free energy approach ($\Delta\nu_c^{\Delta G}$, eq 6). The cosolvent numbering scheme is given in Table 2. The solid line corresponds to a perfect correlation. Error bars are ±1 standard deviation.

Conclusions

We have used a combination of molecular dynamics simulations and Widom particle insertion calculations to determine the salting out constants of helium, neon, argon, and methane in a variety of cosolvents. The free energy differences were small for the cavity sizes studied here, but experimental salting out constants were well reproduced by the calculations. The most significant effects were produced by solutions of sodium chloride, ammonium sulfate, calcium chloride, and TFE. Further examination revealed that the action of sodium chloride and ammonium sulfate salts, although producing very similar effects, corresponded to very different changes in the hydration of the inserted cavities. The presence of sodium chloride did not the change the number of waters in the vicinity of the cavity compared to that in pure water, whereas ammonium sulfate produced a marked increase in the number of waters of hydration. This appeared to be related to the presence of an ammonium sulfate aggregate formed during the simulation. The presence of such aggregates, although speculative and not yet observed experimentally, could help to explain the similarities between the effects of ammonium sulfate and polyethylene glycol on protein stabilization and solubility. It is plausible that ammonium sulfate aggregates, if they exist, may closely resemble the polymeric alcohol in solution.

Concentration dependent hydration effects were also observed for solutions of urea and guanidinium chloride. Denaturing solutions of urea and guanidinium chloride appear to have opposite effects on the hydration of hydrophobic groups: urea increasing the degree of hydration and guanidinium chloride decreasing the degree of hydration. These observations may have a direct bearing on the nature of the denatured state of proteins, especially concerning the degree of exposure of hydrophobic groups on protein denaturation. For instance, the increased hydration of nonpolar groups in urea solution (presumably an unfavorable event), coupled with the stabilization of hydrophobic pair interactions observed in other simulations,[45] may prevent denaturation of the hydrophobic core of many proteins, whereas guanidinium chloride solutions may promote the disruption of both secondary structure and the hydrophobic core. Furthermore,

these results suggest that at low guanidinium chloride concentrations one might not expose the hydrophobic core of a protein, whereas at higher concentrations a favorable cavity−cosolvent interaction could make this process more probable. These latter observations may help to explain some of the conflicting experimental data regarding the nature of the first steps in protein refolding, namely, hydrophobic collapse (Barstar refolded from 6 M guanidinium chloride)[70] vs secondary structure formation (Ribonuclease A refolded from 2.6 M guanidinium chloride).[71] Further investigations into the effects of different concentrations of urea and guanidinium chloride on the aggregation of hydrophobic groups is required to support or refute these possibilities.

Using a preferential binding model, it was possible, with the exception of ammonium sulfate, to correlate the changes in the free energy of solvation with changes in the binding of cosolvent to the inserted cavities for low cosolvent concentrations. Such correlations between thermodynamics and structure provide a powerful tool for the further study of cosolvent effects in these systems.

Appendix

Here we present the equations describing the Widom particle insertion technique when applied to the isothermal isobaric (*N*, *p*, *T*) ensemble. The Widom particle insertion technique provides a route to determine the chemical potential of a species.[72] Originally developed for the canonical ensemble, the technique was extended to include the isothermal isobaric ensemble by Shing and Chung.[55] Slightly different results are obtained if one uses the density of volume states proposed by Attard for the isothermal isobaric ensemble,[73] and therefore we present the results below. The following equations refer to a single component system, although they can be readily generalized for multicomponent systems.[55] Making the usual finite difference approximation for the chemical potential

$$\mu = \left(\frac{\partial G}{\partial N}\right)_{p,T} \approx G(N+1, p, T) - G(N, p, T) = -k_B T \ln\frac{\Delta(N+1, p, T)}{\Delta(N, p, T)} \quad (8)$$

where the isothermal isobaric partition function Δ is given by[73]

$$\Delta(N, p, T) = N\int_0^\infty V^{-1}\, e^{-\beta pV} e^{-\beta A(N,V,T)}\, dV \quad (9)$$

and $A(N, V, T)$ is the Helmholtz free energy,

$$A(N, V, T) = -k_B T \ln\left[\frac{q^N}{N!\Lambda^{3N}}\int_V e^{-\beta U} dr^{3N}\right] \quad (10)$$

with $\beta = (k_B T)^{-1}$, q is the molecular partition function, Λ is the thermal De Broglie wavelength,[74] and U is the configurational energy which depends only on the positions of the particles. It is then possible to show that[55,72]

$$\mu = -k_B T \ln\left[\frac{q}{N\Lambda^3}\langle V e^{-\beta\Delta U}\rangle_{N,p,T}\right] \quad (11)$$

where the angular bracket denotes an ensemble average and ΔU is the change in configurational energy on insertion of the test particle. The above expression can also be written

$$\mu = \mu^{id} - k_B T \ln\left[\frac{\langle V e^{-\beta\Delta U}\rangle_{N,p,T}}{\langle V\rangle_{N,p,T}}\right] \quad (12)$$

with,

$$\mu^{id} = -k_B T \ln\left[\frac{q}{\rho\Lambda^3}\right] \quad (13)$$

This above expression differs from that obtained in the canonical ensemble by the inclusion of the volume term within the ensemble averages. Furthermore, the presence of the density of volume states (N/V) in the isothermal isobaric partition function naturally leads to a definition of the density $\rho = N/\langle V\rangle$, rather than the approximate expression $(N+1)/\langle V\rangle$.[55] Obviously, the latter difference will only be important for small systems, when volume fluctuations are large (phase transitions), or when one requires very high precision results. It is plausible that inclusion of the volume term may be more significant as one can envision a correlation between the system volume and the exponential term in eq 12, i.e., larger volumes would permit more successful insertions. Therefore, the importance of including the volume explicitly when calculating the above free energy differences was tested. For the data presented in Tables 3−6, setting $V = 1$ produces identical results, within the error of the simulations, to those obtained by using the exact expression.

Correspondingly, the enthalpy change associated with particle insertion can be obtained via

$$\Delta H = H(N+1, p, T) - H(N, p, T) = k_B T^2 \left(\frac{\partial \ln[\Delta(N+1, p, T)/\Delta(N, p, T)]}{\partial T}\right)_{N,p} \quad (14)$$

which, assuming $\partial q/\partial T = 0$, leads to the expression

$$\Delta H = 3/2 k_B T + \frac{\langle(\Delta U + H_N) V e^{-\beta\Delta U}\rangle - \langle V e^{-\beta\Delta U}\rangle\langle H_N\rangle}{\langle V e^{-\beta\Delta U}\rangle} \quad (15)$$

where H_N is the enthalpy ($H = U + pV$) in the N particle ensemble and all averages are determined at constant N, p, and T.

The range of validity of the Widom particle insertion technique has been investigated by Beutler et al. by comparing the results for insertion of purely repulsive cavities into SPC water with high precision thermodynamic integration calculation for the same systems.[75] The repulsive cavity was modeled using an r^{-12} potential, and the size of the cavity was described by a thermal radius (r_{th}) which is defined as the distance at which the cavity−water potential equals $k_B T$. Their results suggest that Widom particle insertion techniques reproduce the correct solvation free energy for cavities with $r_{th} \leq 0.3$ nm. As a test of our methods the same calculations were performed in both SPC and SPC/E water. We find that the good agreement between the particle insertion and thermodynamic integration results can be extended to thermal radii of ≈0.4 nm, as long as sufficient insertion attempts are made. For example, our insertion results for cavities with thermal radii of 0.1, 0.2, 0.3, and 0.4 nm into SPC water were 0.5, 5.3, 21.2(2), and 57(2) kJ/mol, respectively, compared to the thermodynamic integration results of 0.5, 5.6, 22.4(3), and 53(1) kJ/mol, respectively.[75] It appears that the increase in the range of success of particle insertion calculations performed here is due to the large number of trial insertions. The reason for this is immediately apparent if one considers the case of inserting a hard sphere solute into a hard sphere solvent. Here, the energy change on insertion is either infinity or zero and the free energy for insertion is given by $-k_B T \ln(n/N)$, where n is the number of successful insertions and N the total number of attempts. A free energy change of 50 kJ/mol

($\approx 20 k_B T$) implies a success rate of 1 in every 2×10^9 attempts. Hence, larger cavities naturally require more particle insertion attempts. The physical picture is of a search for larger, and therefore more transient, cavities in solution.[76,77] Interestingly, insertion of the above cavities into SPC/E water produced solvation free energies of 0.5, 5.5, 22.3(2), and 57(2) kJ/mol, respectively, while Floris et al.[78] recently calculated a value of 56(1) kJ/mol for insertion of a cavity with thermal radius of 4.1 nm into TIP4P water. Hence, there appears to be very little water model dependence for these calculations.[58]

Acknowledgment. This project was partially supported by the Kansas Agricultural Experimental Station (Publication 99-57-J). This material is based upon work supported by the National Science Foundation under Grant EPS-9550487 and matching support from the State of Kansas.

References and Notes

(1) Blokzijl, W.; Engberts, J. B. F. N. *Angew. Chem., Int. Ed. Engl.* **1993**, *32*, 1545−1579.
(2) Tanford, C. *Science* **1978**, *200*, 1012−1018.
(3) Privalov, P. L.; Gill, S. J. *Adv. Protein Chem.* **1988**, *39*, 191−234.
(4) von Hippel, P. H.; Wong, K. *Science* **1964**, *145*, 577−580.
(5) von Hippel, P. H.; Schleich, T. *Acc. Chem. Res.* **1969**, *2*, 257−265.
(6) von Hippel, P. H.; Schleich, T. The effects of neutral salts on the structure and conformational stability of macromolecules in solution. In *Biological Macromolecules*; Timasheff, S. N., Fasman, G. D., Eds.; Marcel Dekker: New York, 1969; Vol 2, pp 417−574.
(7) Franks, F.; Eagland, D. *CRC Crit. Rev. Biochem.* **1975**, *3*, 165−219.
(8) Collins, K. D.; Washabaugh, M. L. *Q. Rev. Biophys.* **1985**, *18*, 323−422.
(9) Timasheff, S. N.; Arakawa, T. Stabilization of protein structure by solvents. In *Protein Structure: A Practical Approach*; Creighton, T. E., Ed.; IRL Press: London, 1989; pp 331−345.
(10) Timasheff, S. N. *Biochemistry* **1992**, *31*, 9857−9864.
(11) Timasheff, S. N. *Curr. Opin. Struct. Biol.* **1992**, *2*, 35−39.
(12) Baldwin, R. L. *Biophys. J.* **1996**, *71*, 2056−2063.
(13) Cacace, M. G.; Landau, E. M.; Ramsden, J. J. *Q. Rev. Biophys.* **1997**, *30*, 241−277.
(14) Schumpe, A. *Chem. Eng. Sci.* **1993**, *48*, 153−158.
(15) Hermann, C.; Dewes, I.; Schumpe, A. *Chem. Eng. Sci.* **1995**, *50*, 1673−1675.
(16) Weisenberger, S.; Schumpe, A. *AIChE J.* **1996**, *42*, 298−300.
(17) Krishnan, C. V.; Friedman, H. L. *J. Solution Chem.* **1974**, *3*, 727−744.
(18) Bustamante, P.; Drago, R. S. *J. Phys. Chem. B* **1997**, *101*, 5002−5009.
(19) Debye, P.; McAulay, J. *Phys. Z.* **1925**, *26*, 22−29.
(20) McDevit, W. F.; Long, F. A. *J. Am. Chem. Soc.* **1952**, *74*, 1773−1777.
(21) Kirkwood, J. G. *Chem. Rev.* **1939**, *24*, 233−251.
(22) Long, F. A.; McDevit, W. F. *Chem. Rev.* **1952**, *51*, 119−169.
(23) Smith, P. E.; Pettitt, B. M. *J. Phys. Chem.* **1994**, *98*, 9700−9711.
(24) Reiss, H. *Adv. Chem. Phys.* **1966**, *9*, 1−84.
(25) Pierotti, R. A. *Chem. Rev.* **1976**, *76*, 717−726.
(26) Shoor, S. K.; Gubbins, K. E. *J. Phys. Chem.* **1969**, *73*, 498−505.
(27) Masterton, W. L.; Lee, T. P. *J. Phys. Chem.* **1970**, *74*, 1776−1782.
(28) Masterton, W. L.; Bolocofsky, D.; Lee, T. P. *J. Phys. Chem.* **1971**, *75*, 2809−2815.
(29) Masterton, W. L. *J. Solution Chem.* **1975**, *4*, 523−534.
(30) Murphy, K. P.; Privalov, P. L.; Gill, S. J. *Science* **1990**, *247*, 559−561.
(31) Lee, B. *Proc. Natl. Acad. Sci. U.S.A.* **1991**, *88*, 5154−5158.
(32) Schellman, J. A. *Biophys. J.* **1997**, *73*, 2960−2964.
(33) Wetlaufer, D. B.; Malik, S. K.; Stoller, L.; Coffin, R. L. *J. Am. Chem. Soc.* **1964**, *86*, 508−514.
(34) Tanford, C. *Adv. Protein Chem.* **1970**, *24*, 1−95.
(35) Roseman, M.; Jencks, W. P. *J. Am. Chem. Soc.* **1975**, *97*, 631−640.
(36) Guillot, B.; Guissani, Y. *J. Chem. Phys.* **1993**, *99*, 8075−8094.
(37) Jorgensen, W. J.; Blake, J. F.; Buckner, J. K. *Chem. Phys.* **1989**, *129*, 193−200.
(38) Straatsma, T. P.; Berendsen, H. J. C.; Postma, J. P. M. *J. Chem. Phys.* **1986**, *85*, 6720−6727.
(39) Nakahar, M.; Wakai, C.; Yoshimoto, Y.; Matubayasi, M. *J. Phys. Chem.* **1996**, *100*, 1345−1349.
(40) Ludemann, S.; Abseher, R.; Schreiber, H.; Steinhauser, O. *J. Am. Chem. Soc.* **1997**, *119*, 4206−4213.
(41) Smith, D. E.; Zhang, L.; Haymet, A. D. J. *J. Am. Chem. Soc.* **1992**, *114*, 5875−5876.
(42) New, M. H.; Berne, B. J. *J. Am. Chem. Soc.* **1995**, *117*, 7172−7179.
(43) Young, W. S.; Brooks, C. L., III. *J. Chem. Phys.* **1997**, *106*, 9265−9269.
(44) Chipot, C.; Kollman, P. A.; Pearlman, D. A. *J. Comput. Chem.* **1996**, *17*, 1112−1131.
(45) Wallqvist, A.; Covell, D. G.; Thirumalai, D. *J. Am. Chem. Soc.* **1998**, *120*, 427−428.
(46) Duffy, E. M.; Kowalczyk, P. J.; Jorgensen, W. J. *J. Am. Chem. Soc.* **1993**, *115*, 9271−9275.
(47) Chipot, C.; Maigret, B.; Pearlman, D. A.; Kollman, P. A. *J. Am. Chem. Soc.* **1997**, *118*, 2998−3005.
(48) Kinoshita, M.; Hirata, F. *J. Chem Phys.* **1997**, *106*, 5202−5215.
(49) Lyubartsev, A. P.; Forrisdahl, O. K.; Laaksonen, A. *J. Chem. Phys.* **1998**, *108*, 227−233.
(50) MacKerell, A. D., Jr.; Bashford, D.; Bellott, M.; Dunbrack, R. L., Jr.; Field, M. J.; Fischer, S.; Gao, J.; Guo, H.; Ha, S.; Joseph, D.; Kuchnir, L.; Kuczera, K.; Lau, F. T. K.; Mattos, C.; Michnick, S.; Ngo, T.; Nguyen, D. T.; Prodhom, B.; Roux, B.; Schlenkrich, M.; Smith, J. C.; Stote, R.; Straub, J.; Wiorkiewicz-Kuczera, J.; Karplus, M. *FASEB J.* **1992**, *6*, A143.
(51) van Gunsteren, W. F.; Berendsen, H. J. C. *Angew. Chem., Int. Ed. Engl.* **1990**, *29*, 992−1023.
(52) Ryckaert, J.-P.; Ciccotti, G.; Berendsen, H. J. C. *J. Comput. Phys.* **1977**, *23*, 327−341.
(53) de Leeuw, S. W.; Perram, J. W.; Smith, E. R. *Proc. R. Soc. London A* **1980**, *373*, 27−56.
(54) Zwanzig, R. W. *J. Chem. Phys.* **1954**, *22*, 1420−1426.
(55) Shing, K. S.; Chung, S. T. *J. Phys. Chem.* **1987**, *91*, 1674−1681.
(56) Wilhelm, E.; Battino, R.; Wilcock, R. J. *Chem. Rev.* **1977**, *77*, 219−262.
(57) Abraham, M. H. *J. Am. Chem. Soc.* **1982**, *104*, 2085−2094.
(58) Guillot, B.; Guissani, Y.; Bratos, S. *J. Chem. Phys.* **1991**, *95*, 3643−3648.
(59) Pearlman, D. A.; Kollman, P. A. *J. Chem. Phys.* **1989**, *90*, 2460−2470.
(60) Lin, C.; Wood, R. H. *J. Phys. Chem.* **1996**, *100*, 16399−16409.
(61) Rajan, R.; Awasthi, S. K.; Bhattacharjya, S.; Balaram, P. *Biopolymers* **1997**, *42*, 125−128.
(62) Kirkwood, J. G.; Buff, F. P. *J. Chem. Phys.* **1951**, *19*, 774−777.
(63) Weast, R. C. *Handbook of Chemistry and Physics*; CRC Press: Cleveland, 1975.
(64) Wyckoff, R. W. G. *Crystal Structures*; John Wiley & Sons: New York, 1965; Vol. 3.
(65) Schlemper, E. O.; Hamilton, W. C. *J. Chem. Phys.* **1966**, *44*, 4498−4509.
(66) Jorgensen, W. L.; Gao, J. *J. Phys. Chem.* **1986**, *90*, 2174−2182.
(67) Cannon, W. R.; Pettitt, B. M.; McCammon, J. A. *J. Phys. Chem.* **1994**, *98*, 6225−6230.
(68) Caminiti, R. *Chem. Phys. Lett.* **1982**, *88*, 103−108.
(69) Ohtaki, H.; Radnai, T. *Chem. Rev.* **1993**, *93*, 1157−1204.
(70) Agashe, V. R.; Shastry, M. C. R.; Udgaonkar, J. B. *Nature* **1995**, *377*, 754−757.
(71) Udgaonkar, J. B.; Baldwin, R. L. *Nature* **1988**, *335*, 694−699.
(72) Widom, B. *J. Phys. Chem.* **1982**, *86*, 869−872.
(73) Attard, P. *J. Chem. Phys.* **1995**, *103*, 9884−9885.
(74) McQuarrie, D. A. *Statistical Mechanics*; Harper & Row: New York, 1976.
(75) Beutler, T. C.; Beguelin, D. R.; van Gunsteren, W. F. *J. Chem. Phys.* **1995**, *102*, 3787−3793.
(76) Pohorille, A.; Pratt, L. R. *J. Am. Chem. Soc.* **1990**, *112*, 5066−5074.
(77) Pratt, L. R.; Pohorille, A. *Proc. Natl. Acad. Sci. U.S.A.* **1992**, *89*, 2995−2999.
(78) Floris, F. M.; Selmi, M.; Tani, A.; Tomasi, J. *J. Chem. Phys.* **1997**, *107*, 6353−6365.
(79) Berendsen, H. J. C.; Grigera, J. R.; Straatsma, T. P. *J. Phys. Chem.* **1987**, *91*, 6269−6271.
(80) Maitland, G. C.; Rigby, M.; Smith, E. B.; Wakeham, W. A. *Intermolecular Forces: Their Origin and Determination*; Clarenden Press: Oxford, 1981.
(81) Jorgensen, W. L.; Madura, J. D.; Swenson, C. J. *J. Am. Chem. Soc.* **1984**, *106*, 6638−6646.
(82) Straatsma, T. P.; Berendsen, H. J. C. *J. Chem. Phys.* **1988**, *103*, 5876−5886.
(83) Singh, U. C.; Brown, F. K.; Bash, P. A.; Kollman, P. A. *J. Am. Chem. Soc.* **1987**, *109*, 1607−1614.
(84) Jorgensen, W. L.; Tirado-Rives, J. *J. Am. Chem. Soc.* **1988**, *110*, 1657−1666.

(85) van Buuren, A. R.; Berendsen, H. J. C. *Biopolymers* **1993**, *33*, 1159−1166.
(86) Clever, H. L. *IUPAC Solubility Data Series*; Pergamon Press: Oxford, 1979; Vol. 1 (Helium and Neon).
(87) Clever, H. L. *IUPAC Solubility Data Series*; Pergamon Press: Oxford, 1980; Vol. 4 (Argon).
(88) Clever, H. L.; Young, C. L. *IUPAC Solubility Data Series*; Pergamon Press: Oxford, 1987; Vol. 27/28 (Methane).